1. Methods

1. Training the Transformer model

1.1 Unsupervised training datasets

a) Homologous sequences of BhrPETase and LCC^{ICCG} were searched for in Uniclust30 (version 2018_08) and the BFD database with HHblits (the number of iterations was set as 4, and other parameters left as default values) using 15 seed sequences in Pfam family PF01083 as queries. All searched sequences were clustered at 90% identity using CD-HIT to obtain 10847 sequences.

b) Since BFD and Uniclust30 were clustered at very low similarity, they may have been undersampled for fitness modelling in very close regions. Previous work by Frazer *et al.*[1] sampled MSA built with more similar proteins to predict disease variants. We also retrieved 15051 sequences belonging to PF01083 from the UniProt database.

1.2 Training details and the prediction of "less-fitted" candidates

To model the fitness distance of sequences, we trained a neural network with an encoder-decoder from starch. We used a Transformer encoder to process input amino acid sequences with absolute position embedding. Unlike other models such as recurrent and convolutional networks, the Transformer made no assumption on sequence ordering and was more powerful at capturing long-distance relationships in sequence because of the attention mechanism (eq. 1):

$$Attention(Q, K, V) = softmax\left(\frac{QK^T}{\sqrt{d_k}}\right)V \quad (1)$$

We applied multi-head self-attention as described by Vaswani *et al.*[2]. The encoder consists of 3 Transformer layers with 8 heads using an embedding size of 512. Based on the encoder embeddings, the decoder generates probabilities of each token. The model was trained with a masked language modelling objective to predict the real amino acid at the masked position. In this study, 40% of tokens were replaced with mask tokens during training. We used the Adam optimizer with a learning rate set to $3e^{-4}$. Models were trained for 20 epochs using a batch size of 32. Residues were filtered by sorting by the logits assigned to the WT amino acid. The top ten residue positions with the highest average scores from the prediction of each model were selected. The average score was calculated using the following equation:

$$\bar{L}_{residue} = \frac{\sum_1^{19}(L_{mi} - L_{wt})}{19} \quad (2)$$

where $\bar{L}_{residue}$ is the average score of the predicted residue position, L_{mi} and L_{wt} are the predicted logits of the single point mutation in the residue position and the wild-type amino acid, respectively. Excluding the duplicated positions, a total of 18 residue positions were generated, among which W104, H164, M166, W190, H191, H218, and F/I243 were suggested to be located on the PET-binding groove. The Transformer model has been made publicly available at https://github.com/Wublab/code-for-

TubroPETase.

2. Design of stabilizing mutations by the GRAPE strategy

The GRAPE strategy reported in our previous study[3] was used to improve the protein stability. The sequence of BhrPETase$^{H218S/F222I}$ was submitted to the GRAPE-WEB online server (https://nmdc.cn/grape-web/). Based on the sequence information of BhrPETase$^{H218S/F222I}$, AlphaFold2[4] was used to predict the structure model. Subsequently, energy calculations with ABACUS[5], FoldX5[6], and Rosetta_cartesian_ddg[7] were used to identify potentially stabilizing point mutations. The DDD algorithm[8] was used to predict the suitable locations for the introduction of disulfide bonds. The thresholds for ABACUS, FoldX, and Rosetta were set to -3.0 AEU, -1.5 kcal/mol and -1.5 REU, respectively.

3. Cloning

Genes encoding BhrPETase from the bacterium HR29 (GenBank accession number: GBD22443), LCC (GenBank accession number: AEV21261), LCC^{ICCG} (LCC$^{F243I/D238C/S283C/Y127G}$), and FastPETase (*Is*PETase$^{D186H/R280A/N233K/R224Q/S121E}$, *Is*PETase GenBank accession number: BBYR01000074) were commercially synthesized with codon optimization for expression in *Escherichia coli* (*E. coli*) BW25113 (DE3) cells. Tfh (GenBank accession number: JN129499), and TfCut2 (GenBank accession number: HG939556) were synthesized with codon optimization for expression in *E. coli* BL21 (DE3) cells, whereas HotPETase (*Is*PETase$^{S121E/D186H/R280A/N233C/S282C/P181V/S207R/S214Y/Q119K/S213E/R90T/Q182M/N212K/R224L/S58A/S61V/K95N/M154G/N241C/K252M/T270Q}$) was synthesized with codon optimization for expression in *E. coli* Rosetta gami-B cells (General Biosystems, Anhui, China). The nucleotide sequences corresponding to the signal peptide of BhrPETase, LCC, LCC^{ICCG}, Thf, and TfCut2 were removed from the synthetic DNA. The synthesized genes for BhrPETase, LCC, LCC^{ICCG}, and FastPETase were cloned into the *Nhe* I and *Xhol* I sites of the pBAD vector and transformed into *E. coli* BW25113 (DE3), whereas the genes for Thf, TfCut2, and HotPETase were cloned into the *Nde* I and *Xhol* I sites of the pET21a vector, and transformed in *E. coli* BL21 (DE3), and *E. coli* Rosetta gami-B, respectively. A list of nucleotide sequences is provided in Table S6.

4. Site-directed mutagenesis

Variants of BhrPETase, LCC^{ICCG}, Tfh, and TfCut2 were constructed using a QuickChange site-directed mutagenesis kit (Agilent Technologies, Santa Clara, CA, USA). The PCR products were incubated with DpnI (New England Biolabs, Ipswich, MA, USA) to digest the original DNA template and then separately transformed into *E. coli* TOP10 cells. The introduced mutations were confirmed by sequencing (Tianyi Huiyuan, Beijing, China).

5. Protein purification

Plasmids containing BhrPETase, LCC, LCC^{ICCG}, FastPETase, and the variants were transformed into *E. coli* BW25113 (DE3) cells that were grown in 2×YT medium at 37 °C to an OD_{600} of ~1.0 and then induced by (0.2 % (*w*/*v*) L-arabinose for 20 h at 20 °C. Tfh, and TfCut2 and the variants were transformed into *E. coli* BL21 (DE3) cells, whereas HotPETase was transformed into *E. coli* Rosetta gami-B cells. Single colonies

of these transformed cells and grown in 2×YT medium at 37 °C to an OD_{600} of ~1.0 and induced by 1 mM isopropyl β-D-thiogalactopyranoside (IPTG) at 20 °C for 20 h. The *E. coli* cells were harvested by centrifugation (10,000 × g, 10 min) and suspended in lysis buffer (50 mM Na_2HPO_4, 100 mM NaCl and 30 mM imidazole, pH 7.5). Cells were disrupted by ultrasonication on ice. The cell extracts were obtained after removing precipitates by centrifugation (13,000 × g, 1 h, 4 °C) and filtration (0.22-μm filter, Millex). The supernatant was then applied to a 5-mL HisTrap HP column (GE Healthcare, Milwaukee, WI, USA). After washing unbound proteins with lysis buffer supplemented with 50 mM imidazole, the target protein was eluted with elution buffer (300 mM imidazole), and then the buffer was exchanged for storage buffer (50 mM Na_2HPO_4, 100 mM NaCl, pH 7.5) using a HiPrep 26/10 Desalting column (GE Healthcare, USA). The purified enzyme was stored at 4 °C. The purified protein concentration was determined by the BCA method.

6. PET depolymerization assay using Gf-PET films

To evaluate the enzyme saturation concentration of various PET hydrolases, the amorphous Gf-PET film (Goodfellow, 250 μm thickness, product number ES301445, ⌀8 mm, roughly 15 mg) was soaked in 500 μL of 1 M potassium phosphate buffer (pH 8.0) with different enzyme loading levels (3-120 μg of purified enzymes) at 65 °C for 6 h.

In other enzyme assays, a similar experimental setup was used. The Gf-PET film (⌀8 mm, roughly 15 mg) was soaked in 500 μL of 1 M potassium phosphate buffer (pH 8.0) with 30 μg of purified enzyme. For mutation screening, the reaction mixture was incubated at 65 °C for 3 h. For comparison of TurboPETase with other PET hydrolases at different temperatures, the reaction mixture was incubated at 40, 50, 65, and 72 °C for 6 h.

The reactions were terminated by heat treatment (100 °C, 10 min). The supernatant obtained by centrifugation (18,000 × g, 5 min) was then analysed by high-performance liquid chromatography (HPLC) to quantify PET monomers released from PET depolymerization. HPLC analyses were performed following a previously reported procedure[3].

7. Depolymerization of untreated postconsumer PET products

PET films from PET containers with less than 15% crystallinity (⌀8 mm, 12-23 mg) were treated by TurboPETase in 800 μL of 1 M potassium phosphate buffer (pH 8.0) with 2 $mg_{enzyme}\ g_{PET}^{-1}$ enzyme loading. PET films from binder clip packaging (⌀8 mm, 8.5 mg), PET bottle (⌀8 mm, 19 mg), chrysanthemum tea container (⌀8 mm, 19 mg), pumpkin powder container (⌀8 mm, 16 mg), and PET strapping (⌀8 mm, 15 mg) or fibres from black PET fibre (15 mg), nonwoven fabric (10 mg), mosquito net (2.6 mg) and textile fabric (8.5 mg) were treated with TurboPETase in 500 μL of 1 M potassium phosphate buffer (pH 8.0) with 2 $mg_{enzyme}\ g_{PET}^{-1}$ enzyme loading. The reaction mixture was incubated at 65 °C for 72 h. After 72 h, fresh enzymes were added to the reactions. Then, the reactions were terminated after 96 h by heat treatment (100 °C, 10 min). The supernatant obtained by centrifugation (18,000 × g, 5 min) was then analysed by HPLC. A large, untreated and transparent postconsumer PET container (food-packing container, roughly 5.5 g) was treated with 0.41 μM (11 mg) TurboPETase in 300 mM potassium

phosphate buffer (pH 8.0) at 65 °C. The whole piece of transparent PET container was fully submerged in 1 L of enzyme solution and completely degraded after 18 h.

8. Depolymerization of pretreated PET bottles and lower-grade products

Postconsumer PET bottles were collected from the garbage collection station in Beijing, China. PET strappings were purchased from Hebei Zhongbang Co., Ltd. (Hebei, China). The bottle and strapping samples were washed three times with 1% SDS, 20% ethanol and deionized water before usage. PET samples were micronized into small flakes using a JZ-T-005 crusher (Shiyan Precision Instruments Co., Ltd., Dongguan, China). The flakes were subsequently amorphized using a twin-screw extruder SY-6219-20/32 (Shiyan Precision Instruments Co., Ltd., Dongguan, China). The set temperatures were 265 °C in the extruder zones, 285 °C in the melt pump, and 285 °C in the screen changer zones. The obtained amorphous micropellets of PET were then micronized by a DingLi flour-mixing machine (DFY-1000D) at room temperature. After sieving, PET powders with particle size less than 400 μm were obtained.

Pretreated PET bottles (16 g and 24 g) and 24 g pretreated postconsumer coloured strapping were treated in 80 mL of 100 mM potassium phosphate buffer (pH 8.0) with 2 mg_{enzyme} g_{PET}^{-1} enzyme loading at 65 °C in a 500 mL bioreactor (Shanghai Kuangsheng Co., Ltd., Shanghai, China). The pH was regulated at 8 by the addition of a 4 N NaOH solution. The conversion was determined by the determination of PET monomers released from PET depolymerization by HPLC, and final conversion was additionally confirmed by residual solid weight measurement.

9. Scanning electron microscopy

The morphology of PET films before and after enzyme exposure was examined following a previously reported procedure[3].

10. Determination of apparent melting temperatures and PET crystallinity

A fluorescence-based thermal stability assay was used to determine apparent melting temperatures. The crystallinity of postconsumer plastic products was analysed by DSC. The parameters were set following a previously reported procedure[3].

11. Kinetics analysis

Initial rate measurements were collected for the ^{conv}MM and ^{inv}MM datasets. For the ^{conv}MM dataset, Gf-PET films over a range of 0-50 g L^{-1} were treated in 300 μL of 1 M potassium phosphate buffer (pH 8.0) with enzyme loadings of 0.12 μM, 0.37 μM and 0.74 μM (1-6 μg). For the ^{inv}MM dataset, 12 g L^{-1}, 20 g L^{-1}, and 30 g L^{-1} Gf-PET films were treated in 500 μL of 1 M potassium phosphate buffer (pH 8.0) with enzyme loading levels ranging from 0-2.67 μM (0-36 μg). The reaction mixture was incubated at 65 °C for 1 h. All reactions were performed in triplicate and terminated by heating to 100 °C for 10 min. The supernatant obtained by centrifugation (18,000 × g, 5 min) was then analysed by HPLC. The data were fitted using Origin Pro 2019.

12. Molecular docking and MD simulations

TurboPETase was modelled by AlphaFold2[4]. Then, the protein was simulated for 20 ns. The representative structure obtained from the equilibrated simulations and the crystal structure of BhrPETase (PDB ID: 7EOA) was used for further docking. A previously reported model substrate was used[3]. Molecular docking was performed by YASARA. The docking model with the highest binding energy and distance of the PET

carbonyl carbon and Ser165 Cα atom below 4 Å were selected and subjected to local docking for 999 runs, yielding the final docked binding mode. The TurboPETase-PET and BhrPETase-PET complexes were simulated in AMBER 16[9] using the ff16SB force field. The His242 residue was protonated in the HID state. The previously reported force field parameters of PET were used[3]. The systems were minimized over 12,000 steps and heated from 0 K to 310 K by Langevin dynamics with a collision frequency of 1 ps^{-1}. After equilibration for 500 ps, 100 ns MD simulations for each complex were performed.

Supplementary Tables

Table S1. Top 10 predicted amino acid positions ranked by the average score predicted by the Transformer model. Residues located on the PET-binding groove are labeled in blue.

Rank	BhrPETase				LCC^{ICCG}			
	Uniclust30 and BFD database		UniProt database		Uniclust30 and BFD database		UniProt database	
	Predicted Residue Position	Average score	Predicted Residue Position	Average score	Predicted Residue Position	Average score	Predicted Residue Position	Average score
1	C275	1.94	C275	3.64	H112	1.99	C275	4.19
2	H112	1.77	Y77	1.98	C275	1.96	Y77	2.02
3	M166	1.64	W104	1.90	H191	1.62	W190	1.97
4	H218	1.34	W190	1.72	C238	1.57	F71	1.77
5	Y39	1.30	M91	1.59	H164	1.53	W104	1.70
6	W190	1.29	Y39	1.51	Y234	1.39	M91	1.67
7	H191	1.21	F56	1.46	M166	1.38	W263	1.49
8	W263	1.11	F71	1.42	W190	1.36	F56	1.41
9	H164	1.10	W263	1.30	Y39	1.33	R47	1.32
10	M91	1.05	F243	1.17	H218	1.25	Y39	1.14

Table S2. Thermostability and specific activity of BhrPETase and LCC^{ICCG} and their H218S/F222I variants.

Mutations	T_m (°C)	Specific activity ($mg_{TAeq.}$ h^{-1} mg_{enzyme}^{-1})
BhrPETase	96	6.98
LCC^{ICCG}	94	6.97
$BhrPETase^{H218S/F222I}$ (M2)	85	18.53
$LCC^{ICCG/H218S/F222I}$	84	13.17

Table S3. Thermostability and specific activity of the 32 experimentally evaluated point mutations corresponding to the predicted amino acid positions (W104, H164, M166, W190, H191 and F243) using BhrPETase M2 as the scaffold.

Mutations	ΔT_m (°C)	Specific activity ($mg_{TAeq.}$ h^{-1} mg_{enzyme}^{-1})
BhrPETase M2	-	18.53
W104L	-13	23.20
W104S	-12.5	20.35
W104C	-12.5	16.09
W104H	-9.5	21.44
W104D	-11.5	17.38
W104R	-10.5	7.02
W104G	-13.5	20.89
H164L	-12.5	0.68
H164S	-6	1.85
H164E	-10	0.13
H164Q	-4.5	3.58
H164F	-11	2.35
M166L	-6	0.78
M166S	2	0.07
M166D	-2	1.81
M166F	-1	1.53
W190L	-7	0.64
W190M	-6.5	0.45
W190S	-8.5	2.06
W190H	-8.5	6.81
W190D	-10	0.37
H191L	-9	1.77
H191M	-7	2.32
H191S	1	2.95
H191D	3	5.71
H191Y	-8	7.89
F243I	-4	23.75
F243S	-2	10.69
F243T	-1	22.50
F243D	1.5	11.40
F243N	0	11.91
F243G	-4	24.92

Table S4. Thermostability and specific activity of the point mutations predicted by ABACUS, FoldX, Rosetta_cartesian_ddg and DDD algorithms using BhrPETase M2 as the scaffold[a].

Mutations	ΔT_m (°C)	Specific activity ($mg_{TAeq.}\ h^{-1}\ mg_{enzyme}^{-1}$)	Predicted algorithm	Predicted energy value
S57P	0	18.75	FoldX	-1.52
S64P	+0.5	15.43	Rosetta	-2.64
T85E	-0.5	19.97	FoldX	-1.51
L102V	-5	14.24	ABACUS	-3.59
H112W	0	18.12	Rosetta	-1.88
F127T	-1	13.03	ABACUS	-5.30
S146V	-0.5	16.37	ABACUS	-3.63
I178H	-1.5	17.39	ABACUS	-4.42
H191D	+3	5.71	ABACUS	-3.60
T192Y	0	17.74	Rosetta	-1.56
Q202V	-9	19.13	ABACUS	-8.19
A209R	+2	20.96	Rosetta	-2.00
D238K	+8.5	18.26	ABACUS	-3.72
S287A	-5	19.29	Rosetta	-1.66
A251C-A281C	+3	18.76	DDD	-

[a]The potentially stabilizing point mutations with biophysical pitfalls, such as the introduction of internal cavities, loss of hydrogen-bonding interactions, or exposure of hydrophobic residues at the surface of the enzyme, were eliminated by visual inspection.

Table S5. Thermostability and specific activity of BhrPETase M2-M6 and the experimentally evaluated variants at W104 and F243 positions using BhrPETase M6 as the scaffold.

Mutations	T_m (°C)	Specific activity ($mg_{TAeq.}h^{-1}$ mg_{enzyme}^{-1})
BhrPETase M2	85	18.53
BhrPETase M2-D238K (M3)	93.5	18.30
BhrPETase M3-A251C/A281C (M5)	95.5	18.18
BhrPETase M5-A209R (M6)	97	17.84
BhrPETase M6-F243T-W104L	84	30.54
BhrPETase M6-F243T-W104H	87.5	27.79
BhrPETase M6-F243T-W104S	85	27.06
BhrPETase M6-F243T-W104G	86	22.56
BhrPETase M6-F243I-W104L	82	27.74
BhrPETase M6-F243I-W104H	85	27.31
BhrPETase M6-F243I-W104S	83.5	28.16
BhrPETase M6-F243I-W104G	83	27.40
BhrPETase M6-F243G-W104L	82.5	29.76
BhrPETase M6-F243G-W104H	86	28.48
BhrPETase M6-F243G-W104S	83	29.97
BhrPETase M6-F243G-W104G	83	25.54

Table S6. Sequences used in this study.

PET hydrolase	Nucleotide sequence
BhrPETase	AGCAATCCGTATCAGCGTGGTCCGAATCCGACACGTAGCGCACTGACC ACCGATGGTCCGTTTAGCGTTGCAACCTATAGCGTTAGCCGTCTGAGC GTTAGCGGTTTTGGTGGTGGTGTTATCTATTATCCGACCGGTACAACCC TGACCTTTGGTGGTATTGCAATGAGTCCGGGTTATACCGCAGATGCAA GCAGCCTGGCATGGCTGGGTCGTCGTCTGGCAAGCCATGGTTTTGTTG TTATTGTGATTAATACCAACAGCCGTCTGGATTTTCCGGATAGCCGTGC AAGCCAGCTGAGCGCAGCACTGAATTATCTGCGTACCAGCAGTCCGA GCGCAGTTCGTGCACGTCTGGATGCAAATCGTCTGGCCGTTGCAGGTC ATAGCATGGGTGGTGGCGCAACCCTGCGTATTAGCGAGCAGATTCCGA CACTGAAAGCCGGTGTTCCGCTGACACCGTGGCATACCGATAAAACC TTTAATACACCGGTTCCGCAGCTGATTGTTGGTGCAGAAGCAGATACC GTTGCACCGGTTAGCCAGCATGCAATTCCGTTTTATCAGAATCTGCCG AGCACCACACCGAAAGTTTATGTTGAACTGGATAATGCGACCCATTTT GCACCGAATAGCCCGAATGCAGCAATTAGCGTTTATACCATTAGCTGG ATGAAACTGTGGGTTGATAATGATACCCGTTATCGTCAGTTTCTGTGCA ATGTTAATGATCCGGCACTGAGCGATTTTCGTAGCAATAATCGTCATTG TCAG
LCC	AGTAACCCGTATCAGCGTGGCCCGAATCCGACCCGTAGTGCCCTGACC GCCGATGGTCCGTTTAGTGTTGCAACCTATACCGTTAGCCGCCTGAGT GTTAGTGGCTTTGGTGGTGGTGTTATTTATTATCCGACCGGTACCAGCC TGACCTTTGGCGGCATTGCAATGAGCCCGGGCTATACCGCCGATGCAA GTAGTCTGGCCTGGCTGGGTCGTCGTCTGGCCAGTCATGGCTTTGTGG TTCTGGTGATTAATACCAATAGCCGCTTTGATTATCCGGATAGCCGCGC CAGTCAGCTGAGTGCCGCCCTGAATTATCTGCGCACCAGCAGCCCGA GTGCCGTGCGTGCTCGTCTGGATGCAAATCGCCTGGCAGTGGCAGGT CATAGCATGGGCGGCGGCGGTACCCTGCGTATTGCAGAACAGAATCCG AGTCTGAAAGCAGCCGTGCCGCTGACCCCGTGGCATACCGATAAAAC CTTTAATACCAGCGTGCCGGTGCTGATTGTTGGCGCAGAAGCAGATAC CGTTGCACCGGTGAGTCAGCATGCAATTCCGTTTTATCAGAATCTGCC GAGCACCACCCCGAAAGTGTATGTGGAACTGGATAATGCAAGCCATTT TGCCCCGAATAGCAATAATGCCGCAATTAGTGTTTATACCATTAGTTGG ATGAAGCTGTGGGTGGATAATGATACCCGCTATCGTCAGTTTCTGTGCA ATGTTAATGATCCGGCACTGAGTGATTTTCGTACCAATAATCGCCATTG CCAG
LCC^{ICCG}	AGTAACCCGTATCAGCGTGGCCCGAATCCGACCCGTAGTGCCCTGACC GCCGATGGTCCGTTTAGTGTTGCAACCTATACCGTTAGCCGCCTGAGT GTTAGTGGCTTTGGTGGTGGTGTTATTTATTATCCGACCGGTACCAGCC TGACCTTTGGCGGCATTGCAATGAGCCCGGGCTATACCGCCGATGCAA GTAGTCTGGCCTGGCTGGGTCGTCGTCTGGCCAGTCATGGCTTTGTGG TTCTGGTGATTAATACCAATAGCCGCTTTGATGGTCCGGATAGCCGCGC CAGTCAGCTGAGTGCCGCCCTGAATTATCTGCGCACCAGCAGCCCGA

	GTGCCGTGCGTGCTCGTCTGGATGCAAATCGCCTGGCAGTGGCAGGT CATAGCATGGGCGGCGGCGGTACCCTGCGTATTGCAGAACAGAATCCG AGTCTGAAAGCAGCCGTGCCGCTGACCCCGTGGCATACCGATAAAAC CTTTAATACCAGCGTGCCGGTGCTGATTGTTGGCGCAGAAGCAGATAC CGTTGCACCGGTGAGTCAGCATGCAATTCCGTTTTATCAGAATCTGCC GAGCACCACCCCGAAAGTGTATGTGGAACTGTGCAATGCAAGCCATAT TGCCCCGAATAGCAATAATGCCGCAATTAGTGTTTATACCATTAGTTGG ATGAAGCTGTGGGTGGATAATGATACCCGCTATCGTCAGTTTCTGTGCA ATGTTAATGATCCGGCACTGTGCGATTTTCGTACCAATAATCGCCATTG CCAG
HotPETase	AACTTCCCCCGTGCCTCGCGCCTTATGCAGGCTGCTGTGCTGGGCGGC CTTATGGCCGTTTCCGCAGCGGCCACCGCGCAGACCAATCCGTATGCG CGCGGCCCCAACCCTACCGCCGCCTCGTTGGAAGCCAGCGCGGGACC CTTTACCGTTCGTAGCTTTACCGTTGCCCGTCCGGTCGGATATGGTGCA GGGACCGTCTATTACCCAACCAATGCAGGCGGCACCGTTGGCGCGATT GCAATCGTCCCCGGGTACACCGCGACTCAAAGCAGCATTAACTGGTG GGGTCCGCGCTTAGCTAGCCATGGCTTTGTGGTTATTACCATCGATACG AACAGCACTCTAGACAAGCCCGAGAGCCGTAGCTCGCAACAGATGGC CGCGCTTCGTCAAGTTGCGAGCTTGAACGGGACCAGCAGTAGCCCGA TTTACGGAAAGGTCGATACTGCCCGCGGGGGTGTGATGGGCTGGTCA ATGGGGGGCGGCGGTTCACTTATTAGCGCCGCGAACAACCCGAGTTTA AAAGCAGCGGCAGTCATGGCGCCATGGCATTCTTCAACCAACTTCAG CAGTGTTACCGTGCCGACGCTGATTTTCGCGTGCGAGAATGATAGAAT TGCACCGGTGAAGGAGTATGCGCTGCCGATTTATGATAGCATGTCCCT CAACGCAAAACAGTTTCTGGAAATTTGCGGCGGTAGCCACTCTTGTG CCTGCTCTGGGAACAGCAACCAGGCACTGATCGGAATGAAAGGGGTT GCATGGATGAAACGATTCATGGATAATGACACCCGTTACTCACAGTTC GCCTGTGAGAATCCCAACAGCACAGCCGTGTGCGATTTTCGCACCGC GAACTGTTCC
FastPETase	AACTTCCCCCGTGCCTCGCGCCTTATGCAGGCTGCTGTGCTGGGCGGC CTTATGGCCGTTTCCGCAGCGGCCACCGCGCAGACCAATCCGTATGCG CGCGGCCCCAACCCTACCGCCGCCTCGTTGGAAGCCAGCGCGGGACC CTTTACCGTTCGTAGCTTTACCGTTAGCCGTCCGTCCGGATATGGTGCA GGGACCGTCTATTACCCAACCAATGCAGGCGGCACCGTTGGCGCGATT GCAATCGTCCCCGGGTACACCGCGCGTCAAAGCAGCATTAAGTGGTG GGGTCCGCGCTTAGCTAGCCATGGCTTTGTGGTTATTACCATCGATACG AACAGCACTCTAGACCAGCCCGAGAGCCGTAGCTCGCAACAGATGGC CGCGCTTCGTCAAGTTGCGAGCTTGAACGGGACCAGCAGTAGCCCGA TTTACGGAAAGGTCGATACTGCCCGCATGGGTGTGATGGGCTGGTCAA TGGGGGGCGGCGGTTCACTTATTAGCGCCGCGAACAACCCGAGTTTA AAAGCAGCGGCACCGCAGGCGCCATGGCATTCTTCAACCAACTTCAG CAGTGTTACCGTGCCGACGCTGATTTTCGCGTGCGAGAATGATAGCAT TGCACCGGTGAACAGCAGTGCGCTGCCGATTTATGATAGCATGTCCCA GAACGCAAAACAGTTTCTGGAAATTAAGGGCGGTAGCCACTCTTGTG

	CCAACTCTGGGAACAGCAACCAGGCACTGATCGGAAAAAAAGGGGT TGCATGGATGAAACGATTCATGGATAATGACACCCGTTACTCAACCTT CGCCTGTGAGAATCCCAACAGCACAGCCGTGTCGGATTTTCGCACCG CGAACTGTTCC
Tfh	GCCAACCCCTACGAGAGGGGCCCCAACCCCACCGACGCCCTGCTGGA GGCCAGGAGCGGCCCCTTCAGCGTGAGCGAGGAGAGGGCCAGCAGG TTCGGCGCCGACGGCTTCGGCGGCGGCACCATCTACTACCCCAGGGA GAACAACACCTACGGCGCCGTGGCCATCAGCCCCGGCTACACCGGCA CCCAGGCCAGCGTGGCCTGGCTGGGCGAGAGGATCGCCAGCCACGG CTTCGTGGTGATCACCATCGACACCAACACCACCCTGGACCAGCCCG ACAGCAGGGCCAGGCAGCTGAACGCCGCCCTGGACTACATGATCAAC GACGCCAGCAGCGCCGTGAGGAGCAGGATCGACAGCAGCAGGCTGG CCGTGATGGGCCACAGCATGGGCGGCGGCGGCACCCTGAGGCTGGCC AGCCAGAGGCCCGACCTGAAGGCCGCCATCCCCCTGACCCCCTGGCA CCTGAACAAGAACTGGAGCAGCGTGAGGGTGCCCACCCTGATCATCG GCGCCGACCTGGACACCATCGCCCCCGTGCTGACCCACGCCAGGCCC TTCTACAACAGCCTGCCCACCAGCATCAGCAAGGCCTACCTGGAGCT GGACGGCGCCACCCACTTCGCCCCCAACATCCCCAACAAGATCATCG GCAAGTACAGCGTGGCCTGGCTGAAGAGGTTCGTGGACAACGACACC AGGTACACCCAGTTCCTGTGCCCCGGCCCCAGGGACGGCCTGTTCGG CGAGGTGGAGGAGTACAGGAGCACCTGCCCCTTC
TfCut2	GCGAACCCGTACGAGCGTGGTCCGAACCCGACCGATGCGCTGCTGGA AGCGCGTAGCGGTCCGTTTAGCGTGAGCGAGGAAAACGTTAGCCGTC TGAGCGCGAGCGGTTTTGGTGGCGGTACCATCTACTATCCGCGTGAGA ACAACACCTACGGTGCGGTGGCGATTAGCCCGGGCTATACCGGTACCG AGGCGAGCATTGCGTGGCTGGGTGAACGTATTGCGAGCCACGGTTTT GTGGTTATCACCATTGATACCATCACCACCCTGGACCAGCCGGATAGC CGTGCGGAACAACTGAACGCGGCGCTGAACCACATGATCAACCGTGC GAGCAGCACCGTGCGTAGCCGTATTGACAGCAGCCGTCTGGCGGTTAT GGGTCACAGCATGGGCGGTGGCGGTAGCCTGCGTCTGGCGAGCCAGC GTCCGGATCTGAAAGCGGCGATCCCGCTGACCCCGTGGCACCTGAAC AAAAACTGGAGCAGCGTGACCGTTCCGACCCTGATCATTGGTGCGGA CCTGGATACCATCGCGCCGGTGGCGACCCATGCGAAGCCGTTTTACAA CAGCCTGCCGAGCAGCATCAGCAAAGCGTATCTGGAGCTGGATGGTG CGACCCACTTTGCGCCGAACATTCCGAACAAGATCATTGGTAAATACA GCGTGGCGTGGCTGAAGCGTTTCGTTGACAACGATACCCGTTATACCC AATTTCTGTGCCCGGGTCCGCGTGATGGTCTGTTTGGTGAAGTTGAGG AATATCGTAGCACCTGCCCGTTC

Supplementary Figures

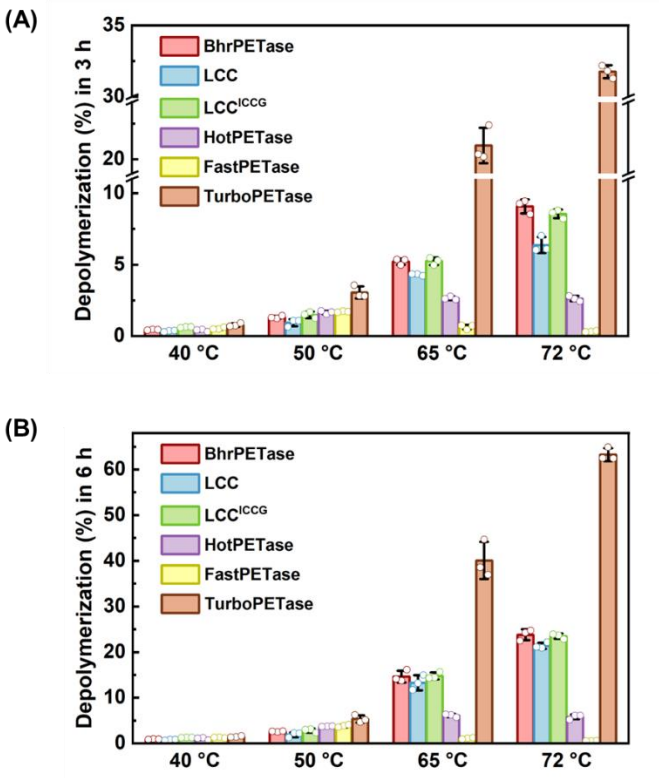

Figure S1. Comparison of the depolymerization performance of BhrPETase, LCC and LCC^{ICCG}, HotPETase, FastPETase, and TurboPETase towards amorphous Gf-PET films (⌀8 mm, 15 mg) for (A) 3 h and (B) 6 h, at reaction temperatures ranging from 40 to 72 ℃. The enzyme loadings were as follows: BhrPETase, LCC, LCC^{ICCG}, and TurboPETase, 2 $mg_{enzyme}\ g_{PET}^{-1}$; HotPETase and FastPETase, 7 $mg_{enzyme}\ g_{PET}^{-1}$. All measurements were conducted in triplicate (n = 3).

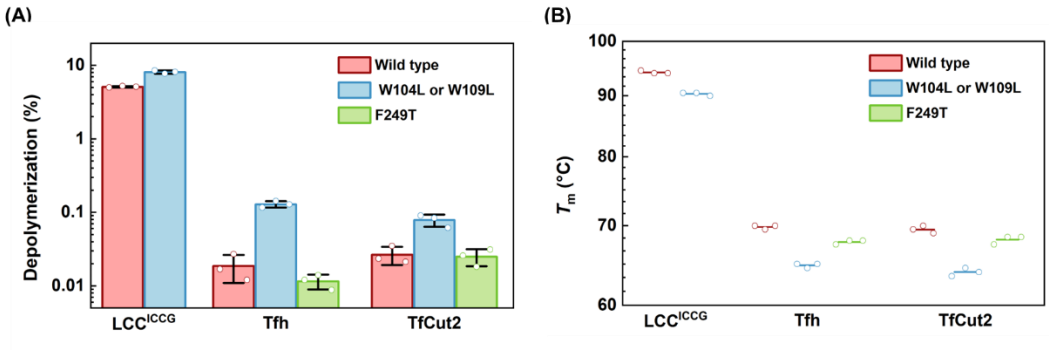

Figure S2. The generalizability of the predicted active mutations in alternative PET hydrolases. (A) Depolymerization of Gf-PET films (⌀8 mm, 15 mg) by wild type PET hydrolases and the variants. Reactions were performed in 500 μL of 1 M potassium phosphate buffer (pH 8.0) for 3 h with 2 mg_{enzyme} g_{PET}^{-1} enzyme loading. The reaction temperatures for each group of enzymes were as follows: LCC^{ICCG}, 65 ℃; Tfh, 50 ℃ and TfCut2, 50 ℃. (B) T_m of wild type PET hydrolases and the variants. All measurements were conducted in triplicate (n = 3). The bars and lines shown for each enzyme represent the average numbers, whereas the circles represent the individual numbers, respectively.

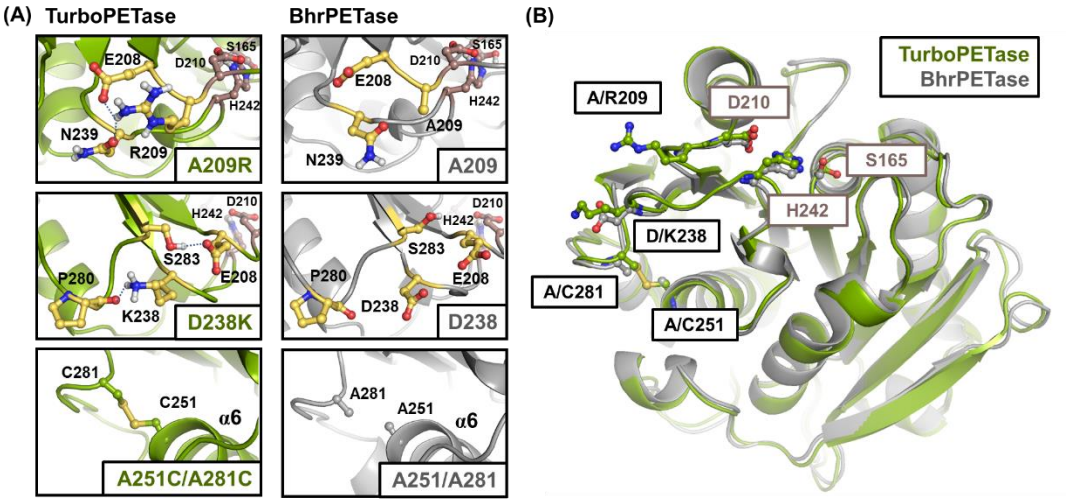

Figure S3. (A) Proposed structural effects of A209R, D238K, and A251C/281C in TurboPETase. A209R may form new salt-bridge interactions with E208 and the guanidine group also donated a new hydrogen bond to the amide oxygen atom of N239. For the D238K mutation, substitution of lysine may decrease the strength of repulsive electrostatic interactions that was evident between native D238 and nearby E208, and the ε-amino group of lysine also pointed towards the backbone oxygen atom of P280 to confer a new hydrogen bond. The A251C/281C disulfide bond was suggested to stabilize the flexible C terminus and the α6 helix. The representative structures were obtained from MD simulations of TurboPETase-PET complex and BhrPETase-PET complex, respectively. Key residues proximal to the stabilizing mutations are colored in yellow and the catalytic triad is colored in darksalmon. (B) Location of the stabilizing mutations. Stabilizing mutations are shown in ball and stick representations.

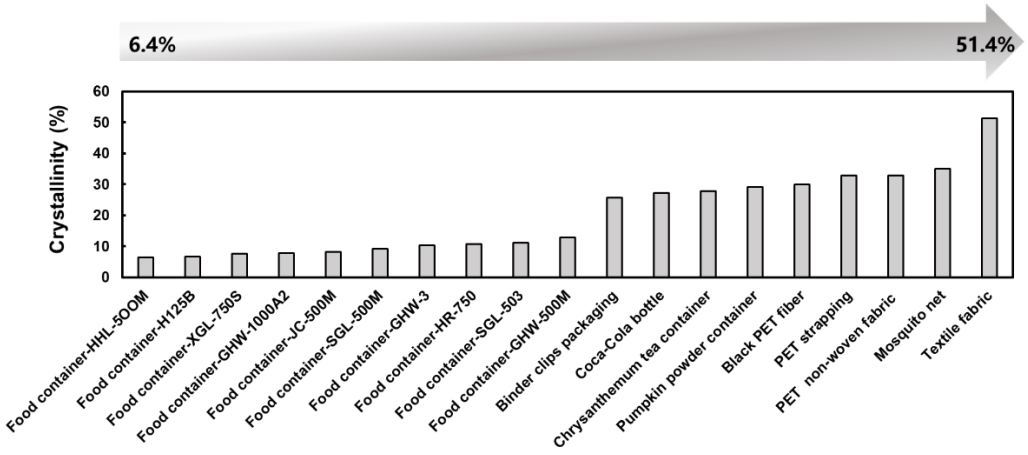

Figure S4. The crystallinity of the postconsumer PET products

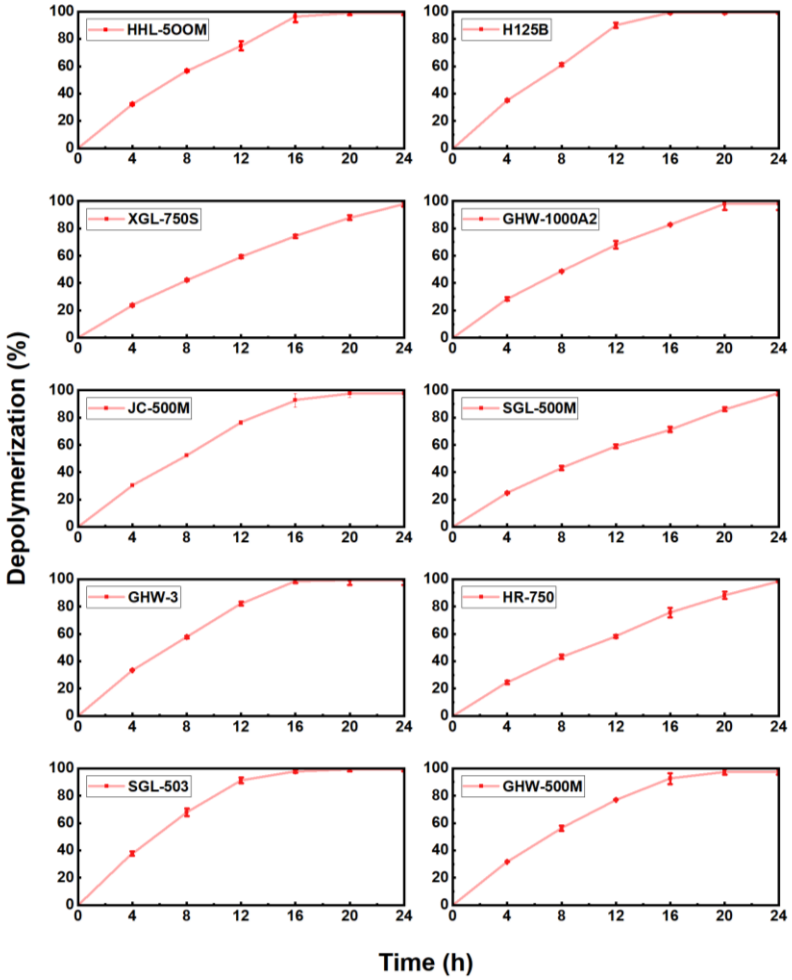

Figure S5. Nearly complete depolymerization of the untreated PET container films with less than 15% crystallinity. The PET samples were treated by TurboPETase in 800 μL of 1 M potassium phosphate buffer (pH 8.0) at 65 ℃ with 2 mg_{enzyme} g_{PET}^{-1} enzyme loading. All measurements were conducted in triplicate (n = 3).

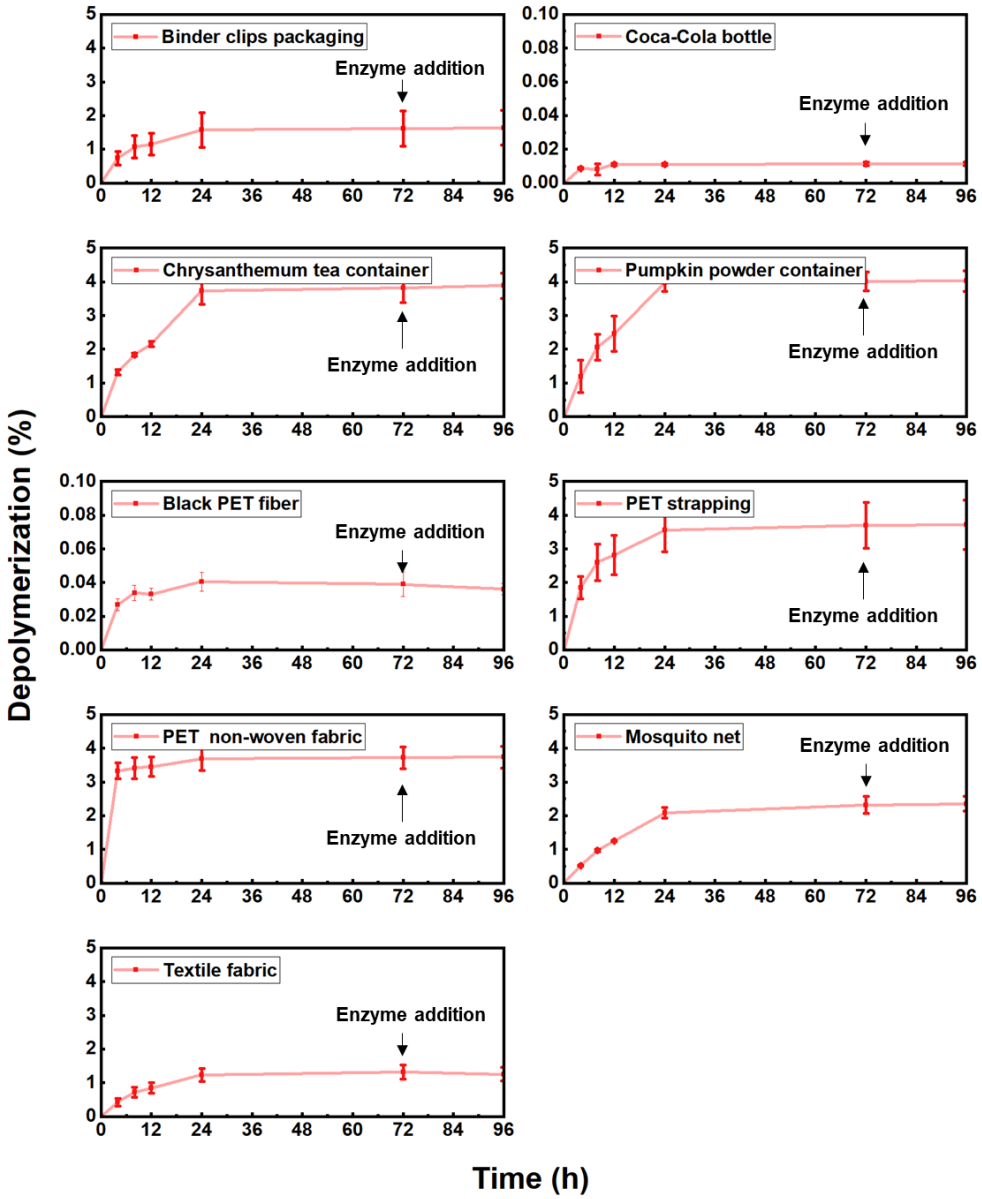

Figure S6. Depolymerization of the untreated postconsumer PET products with high degree of crystallinity above 20%. The PET samples were treated by TurboPETase in 500 μL of 1 M potassium phosphate buffer (pH 8.0) at 65 ℃ with 2 mg_{enzyme} g_{PET}^{-1} enzyme loading. Addition of fresh enzymes after 72 h did not give rise to additional products. All measurements were conducted in triplicate (n = 3).

References

1. Frazer, J., et al. Disease variant prediction with deep generative models of evolutionary data. *Nature* **599**, 91-95 (2021).
2. Vaswani, A., et al. Attention is all you need. *Adv. Neural. Inf. Process. Syst.* 30 (2017).
3. Cui, Y. *et al.* Computational redesign of a PETase for plastic biodegradation under ambient condition by the GRAPE strategy. *ACS Catal.* **11**, 1340-1350 (2021).
4. Jumper, J., et al. Highly accurate protein structure prediction with AlphaFold. *Nature*, **596**, 583-589 (2021).
5. Xiong, P. *et al.* Protein design with a comprehensive statistical energy function and boosted by experimental selection for foldability. *Nat. Commun.* **5**, 5330 (2014).
6. Delgado, J., Radusky, L. G., Cianferoni, D. & Serrano, L. FoldX 5.0: working with RNA, small molecules and a new graphical interface. *Bioinformatics* **35**, 4168-4169 (2019).
7. Park, H. *et al.* Simultaneous optimization of biomolecular energy functions on features from small molecules and macromolecules. *J. Chem. Theory Comput.* **12**, 6201-6212 (2016).
8. Arabnejad, H. *et al.* A robust cosolvent-compatible halohydrin dehalogenase by computational library design. *Protein Eng. Des. Sel.* **30**, 173-187 (2017).
9. Case, D., Darden, T., Cheatham, T., Simmerling, C., Wang, J. & Duke, R. AMBER 14, University of California, San Francisco. 2014.